Is Dynamic Autocrine Insulin Signaling Possible? A Mathematical Model Predicts Picomolar Concentrations of Extracellular Monomeric Insulin within Human Pancreatic Islets

Minghu Wang[1], Jiaxu Li[1]*, Gareth E. Lim[2], James D. Johnson[2]*

1 Department of Mathematics, University of Louisville, Louisville, Kentucky, United States of America, 2 Department of Cellular and Physiological Sciences and Department of Surgery, University of British Columbia, Vancouver, BC, Canada

Abstract

Insulin signaling is essential for β-cell survival and proliferation *in vivo*. Insulin also has potent mitogenic and anti-apoptotic actions on cultured β-cells, with maximum effect in the high picomolar range and diminishing effect at high nanomolar doses. In order to understand whether these effects of insulin are constitutive or can be subjected to physiological modulation, it is essential to estimate the extracellular concentration of monomeric insulin within an intact islet. Unfortunately, the *in vivo* concentration of insulin monomers within the islet cannot be measured directly with current technology. Here, we present the first mathematical model designed to estimate the levels of monomeric insulin within the islet extracellular space. Insulin is released as insoluble crystals that exhibit a delayed dissociation into hexamers, dimers, and eventually monomers, which only then can act as signaling ligands. The rates at which different forms of insulin dissolve *in vivo* have been estimated from studies of peripheral insulin injection sites. We used this and other information to formulate a mathematical model to estimate the local insulin concentration within a single islet as a function of glucose. Model parameters were estimated from existing literature. Components of the model were validated using experimental data, if available. Model analysis predicted that the majority of monomeric insulin in the islet is that which has been returned from the periphery, and the concentration of intra-islet monomeric insulin varies from $\sim$50–300 pM when glucose is in the physiological range. Thus, our results suggest that the local concentration of monomeric insulin within the islet is in the picomolar 'sweet spot' range of insulin doses that activate the insulin receptor and have the most potent effects on β-cells *in vitro*. Together with experimental data, these estimations support the concept that autocrine/paracrine insulin signalling within the islet is dynamic, rather than constitutive and saturated.

Introduction

There is increasing evidence that insulin has critical autocrine or paracrine feedback actions within pancreatic islets [1], [2]. There are also data that suggests that human islets may undergo insulin resistance in type 2 diabetes [3], potentially unifying the etiology of type 2 diabetes. Two lines of evidence have been presented that suggest that β-cell insulin signaling is physiologically relevant. First, *in vivo* loss-of-function studies demonstrate that β-cell insulin signaling plays an important role in the control of β-cell apoptosis, proliferation and mass. For example, Kulkarni's group has shown that knockout of the β-cell insulin receptor reduced functional β-cell mass and increased apoptosis [4],[5],[6],[7]. Moreover, the same group has demonstrated that β-cell proliferation in response to both genetic and diet-induced insulin resistance was absent in mice lacking β-cell insulin receptors [8]. Our observation that physiolog-

ical hyperinsulinemia is required for the high fat diet-induced increase in β-cells implies sensitivity to dynamic changes in insulin [9]. Complementing these *in vivo* loss-of-function studies, we and others have shown that exogenous insulin protects primary human and mouse islet cells from serum-withdrawal-induced apoptosis, via NAADP-dependent Ca^{2+} release, a signalling hub involving 14-3-3ζ, Raf1, Mek, Erk, and Bad, as well as master transcription factors such as Pdx1 and Foxo1 [10],[11],[12],[13],[14]. We also showed that insulin, but not glucose, directly increases proliferation of primary mouse dispersed islet β-cells [15]. These observations complement the work of multiple groups that suggest that insulin promotes β-cell survival. Whether insulin can affect β-cell secretory function or protein synthesis acutely is more controversial [16] and may depend on the dose, duration and context of the insulin signal [17].

Perhaps the most unexpected observation of our previous studies was that the dose-response relationships between insulin and apoptosis or proliferation did not follow a typical dose-response relationship [1]. We have consistently observed that lower doses of insulin, typically 200 pM, were more effective than higher doses in the nanomolar range [10],[11],[12],[13],[18]. However, the *in vivo* relevance of signaling events activated by picomolar insulin doses has been questioned due to the speculative assumption that β-cells are exposed to extremely high levels of insulin within the islet. Although it may seem intuitive to some that local insulin levels would be high near the β-cell, there is no direct evidence for this. The insulin concentration in the native β-cell microenvironment has never been measured experimentally. The physically closest insulin measurements to the islet *in vivo* are those of the portal vein (400–1200 pM depending on the glucose concentration) [19], but this represents the net insulin release from ∼1 million islets dispersed throughout the pancreatic parenchyma (40 cm^3) [20] concentrated into the relatively small volume of a single vein. Moreover, there are two important clues that support the possibility that β-cells may be exposed to insulin concentrations less than that of the portal circulation. First, some β-cells must be exposed to circulating blood first, before other cells, within the complex microvasculature of the islet [10],[21], and would therefore be exposed to insulin levels identical to non-endothelial cells bathed by the peripheral circulating insulin, which is 40–100 pM at rest and 400 pM after a meal [19]. Second, it is known that insulin is stored and secreted as an insoluble microcrystal, dissolving only when exposed to the pH of blood [22]. This means that the amount of local monomeric insulin capable of binding to β-cell receptors depends on both the secretion rate and the rate at which insulin crystals dissolve into active monomers. There is also the argument that β-cells would be optimally tuned to the range of insulin they see *in vivo*, and we have shown they are most responsive at ∼200 pM [10],[11],[12],[13],[18]. Insulin binding assays have shown that the IC50 of the ligand for the insulin receptor is in the picomolar range (88 pM) [23]. Given the current hurdles to experimentally measure the intra-islet insulin concentration, a powerful alternate approach is to undertake quantitative estimates using mathematical modeling [24]. We expect that the technology to measure insulin monomer levels *in vivo* will eventually be developed and permit our predictions to be tested experimentally.

An accurate model to distinguish the contribution of peripheral insulin and newly secreted insulin on β-cell dynamics requires detailed knowledge of a number of key parameters, including the rate of insulin secretion and the rate by which insulin crystals convert to monomers. In this work, local insulin refers to the newly synthesized and released insulin while peripheral insulin refers to insulin in circulating blood re-entering islets. The insulin surrounding the β-cell is therefore a blend of these two concentrations. After synthesis, insulin is packaged in dense-core secretory granules as an insoluble zinc-associated crystal and is released following Ca^{2+}-dependent exocytosis in response to glucose [22],[25]. At high concentrations, such as those contained in therapeutic insulin formulations, insulin is primarily aggregated into hexamers as the default state [26]. Two sequential steps are required for the dissolution of the released insulin crystal into monomers, which interact with their cognate receptors. Each insulin hexamer must first dissolve into three dimers, followed by the breakdown into six insulin monomers [26],[27],[28]. With these delays, a fraction of non-monomeric insulin may flow and/or diffuse away from the immediate vicinity of the β-cells. Therefore, the concentration of the local monomeric insulin that contributes to active signaling could be lower than the total insulin released.

Mathematical modeling is therefore an important in silico tool for biologists to better understand the properties and actions of insulin *in vivo* in sites where it cannot be measured directly. Here, we report the outputs from the first such model, which illustrates the possible kinetics of the endogenous local insulin near β-cells. This work provides new insight into whether signaling events activated by high picomolar insulin might be relevant *in vivo*.

Results

Model formulation and logical considerations

The islets of Langerhans are clusters of 50–1000 endocrine cells. They are dispersed throughout the pancreas and represent 1–2% of the total pancreatic volume. Pancreatic islets are highly vascularized micro-organs, with a central core of β-cells surrounded by other endocrine cells, although this organization is less strict in adult human islets [21] or >1 year-old adult mouse islets [29]. Insulin secreting β-cells comprise the majority (∼50–70%) of islet endocrine cell types, although this can depend on the islet and on the individual [30]. A pancreatic islet is composed of ∼65% endocrine cells, and ∼35% extracellular space/vasculature [31].

The present model is built on the logical assumption that the kinetics by which insulin crystals dissolve plays a critical role in the local islet insulin concentration. The release of intact insulin crystals from single β-cells has been demonstrated by multiple groups (e.g. Fig. 3I, in reference [22]), and it follows that it must take some time for these crystals to dissipate after exocytosis (Fig. 4F in reference [22]). The rate at which insulin hexamers dissolve into dimers and then monomers after subcutaneous injection at a point source has previously been addressed by our group and others (Fig. 1 in Li and Kuang [27]) and it happens on a time-scale of hours [26], [32]. The *in vivo* half-life of insulin is known to be 5–6 minutes [33], which means virtually all of the body's insulin must be replaced by the 1 million islets in ∼10 minutes. The baseline peripheral insulin concentration in the whole body circulation is 50–80 pM. While we are not aware of studies that have directly measured insulin levels in arteries flowing into the pancreas, one would assume that non-degraded peripheral insulin returns to the pancreas at concentrations similar to any other organ. In addition to the prominent insulin degradation in the periphery, we also expect significant insulin re-uptake and degradation in islets, since β-cells are highly enriched with insulin receptors [12] and the endocytosis of insulin: insulin receptor complexes leads to their degradation in lysosomes (T. Albrecht, J.D. Johnson, unpublished data).

We initially considered whether the rate of blood flow in the pancreas might also be an important component of the model. Arterial blood flows into the pancreas through an artery connected to the aorta and flows out of the pancreas via the portal vein after passing through a network of fine capillaries. Although it was originally though that islet blood flow always proceeded from the inside out, recent *in vivo* imaging of intra-islet blood flow in mice has revealed multiple patterns of local islet blood flow (Fig. 5 in Meier et al. [21],[34]). There is also evidence that blood can fill some whole islets evenly without a flow direction (Fig. 4 of Nyman et al. [21]). Regardless of the direction, each case will have some 'prime' or 'upstream' β-cells exposed to fresh arterial blood with other β-cells subsequently exposed to locally released insulin. The percentage of β-cells exposed to fresh arterial blood is related to the width of an islet, which is relatively uniform and conserved throughout evolution. For simplicity, we will assume that, on average, the blood flow in the islet is irregular relative to the location of a given β-cell. Islet capillaries have been shown by
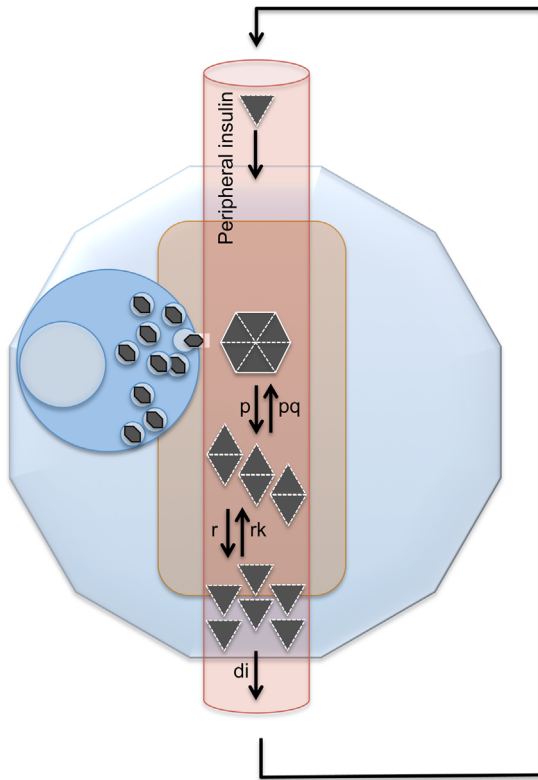
Figure 1. Model diagram for estimation of islet insulin concentration of hexamers, dimers, and monomers. This diagram reflects that, in an intact pancreatic islet, newly synthesized and released hexameric insulin dissolves into dimers and then monomers. Newly released insulin moves out of pancreas into peripheral circulation and then returns the islet with blood flow as 'old' peripheral insulin.
doi:10.1371/journal.pone.0064860.g001

electron microscopy to possess very thin endothelial cells, which are highly fenestrated and permeable [35], suggesting that the local barriers to the movement of insulin crystals, hexamers or dimers are negligible. For the sake of simplicity, this initial model will therefore not consider physical barriers between the β-cell and the circulation. Newly released insulin flows out of the pancreas and into the liver through the hepatic portal vein within a few seconds. The mean portal vein blood flow rate has been measured between 0.8 and 1.1 L/min, and no changes are observed between the basal state and a hyperglycemic clamp [19]. The total rate of pancreatic blood flow through the entire pancreas has been estimated using computed tomography to be 1.5 ml/min per ml of pancreas tissue [36]. Since we only consider a single prototypical islet as the point source in this model, and blood flow does not need to be considered, as its rate is relatively constant in and out of the islet. In other words, the dilution of 'islet blood' with re-circulating insulin in peripheral blood cancels out the addition of new insulin to the blood downstream of the islet.

All of the above considerations are summarized in the single islet model diagram (Fig. 1). These can also be summarized in the following word equation system for this model that considers a single islet and follows the law of mass action and the law of conservation. The rate of change of the concentration of insulin in any form can be expressed as the

$$\text{Rate of Change} = \text{Input Rate} - \text{Output Rate}.$$

We denote the concentration of insulin hexamers by H (in pM), dimers by D (in pM), monomers by M (in pM), and peripheral insulin monomers returned to the islet by I (in pM). The transfer of peripheral insulin monomers should be same as the monomeric insulin concentration that remains in the circulation. We therefore obtain the following model for relative concentrations of local free insulin hexamers, dimers and monomers, and peripheral insulin:

$$\begin{cases} H' = f(G_0)/6 - p(H - qD^3) \\ D' = p(H - qD^3) - r(D - kM^2) \\ M' = r(D - kM^2) - d_i M \\ I' = \alpha M - d_i I \end{cases} \quad (1)$$

with the initial condition $H(0) = H_0 \geq 0$, $D(0) = D_0 \geq 0$, $M(0) = M_0 \geq 0$, $I(0) = I_0 \geq 0$. The transport from newly secreted insulin to peripheral insulin is assumed to be proportional to the level of monomers, $g(M) = \alpha M$, $\alpha > 0$, and the secretion of insulin hexamers is stimulated by glucose, which follows the dynamics of Hill's function $f(G) = \dfrac{\sigma G^n}{a^n + G^n}$, which has been employed in other models [27], [37], [38], [39], [40], [41]. The division of $f(G_0)$ by 6 is due to the secretion of insulin from the β-cells as insulin hexamers. All parameters have the following meanings.

p (min^{-1}) – the dissolution rate from hexamer to dimer.

q (L^2/pmol^2) – the coefficient of the aggregation from dimer to hexamer.

r (min^{-1}) – the dissolution rate from dimer to monomer. It is faster for a dimer to dissolve into two monomers than for a hexamer to dissolve into three dimers. Hence $r > p$.

k (L/pmol) – the coefficient of the aggregation from monomer to dimer.

G_0 (mM) – the clamped glucose concentration (normal *in vivo* range is 3.9–6.1 mM).

d_i (min^{-1}) – the degradation rate of insulin (both local free and peripheral).

σ (pM/min/mM) – maximum secretion rate of insulin stimulated by glucose.

α (min^{-1}) – the transfer rate of newly secreted insulin to peripheral insulin.

a (mM) – half-saturation point in Hill's function $f(G)$.

Model analysis

Next, we studied the qualitative behaviors of the model (1). The model has a unique equilibrium $E^* = (H^*, D^*, M^*, I^*)$, given by

$$M^* = \frac{c}{d_i}, \quad I^* = \frac{\alpha M^*}{d_i}, \quad D^* = \frac{c}{r} + kM^{*2}, \quad H^* = \frac{c}{p} + qD^{*3}, \quad (2)$$

where $c = f(G_0)/6$. Since the system (1) is cooperative, it is intuitive that the unique equilibrium is globally stable. To this end, we first obtain the following:

Theorem 1 *Any solution of the model (1) with initial condition, $H_0 \geq 0, D_0 \geq 0, M_0 \geq 0, I_0 \geq 0$, is positive and bounded.*

The proof of this analytical result can be found below. Then, with direct application of Theorem 1, and Theorem 2.3.1 (in

Smith, HL, page 8 of reference [42]), we obtain the following theorem that qualitatively ensures the reliability and robustness of our model. In next section we further demonstrate that our numerical analysis is quantitatively reasonable.

Theorem 2 *The unique equilibrium point E^* is globally asymptotically stable.*

It can be seen by (2) that, at equilibrium, the concentrations of local insulin M, peripheral insulin I, hexamers and dimers depend on G_0 in nonlinear relationships. However, the ratio of the newly synthesized insulin and the peripheral insulin at equilibrium can be expressed by

$$\frac{M^*}{I^*} = \frac{d_i}{\alpha}. \tag{3}$$

The equation (3) indicates that the ratio of the concentration of local free insulin and peripheral insulin is linearly dependent on insulin degradation d_i, and inversely proportional to the transfer rate α. On the other hand, insulin concentration of intra-islet can be estimated by

$$M^* = \frac{d_i I^*}{\alpha}. \tag{4}$$

Parameter estimation and numerical simulations

As detailed in the following section, model parameters were selected based on the existing literature, regression fitting of experimental data found in the literature, or reasonable assumptions from known physiological principles. Using the resulting model, we then simulated insulin secretion dynamics under conditions of various clamped glucose inputs. We chose the initial condition of the model as $H(0)=0, D(0)=0, M(0)=0$, and $I(0)=0$ as Theorem 2 guarantees that the equilibrium is globally stable and thus the initial conditions do not affect the equilibrium.

The estimation of insulin secretion rate $f(G)$ was as follows. It is widely accepted that the insulin secretion response to glucose takes a sigmoid shape function, namely Hill's function $f(G) = \dfrac{\sigma G^2}{a^2 + G^2}$. To estimate the parameters σ, a and n, we primarily used published data of *in vivo* insulin secretion rates at various glucose levels in human subjects [43], [44] as shown in following Table 1 by employing the Least Square Method. Additional points on the curve were estimated and added for fitting. The fitting results in $\sigma=111.96, a=9.34$ and $n=3.15$. Panel (B) in Fig. 2 illustrates the fitted curve. It is noteworthy that the estimated values are in agreement to those estimated in IVGTT models ([37], [38], [39]). As mentioned earlier, this secretion rate should be divided by 6 to obtain the secreted concentration of insulin hexamers.

The estimation of p and q was as follows. We estimated the values of the parameters p and q for human insulin based on data from insulin analogues, with the assumption that the dissolution and aggregation rates of human insulin falls between the rates associated with fast insulin analogues and slow insulin analogues. According to Li and Kuang, 2009 [27]; Tarin et al 2005 [45] and Trajanoski et al 1993 [32], the value of the parameter p (min^{-1}) remains the same for fast and slow insulin analogues. So we assume that $p=0.5$ (min^{-1}) for human insulin as well. Table 2, adopted from Tarin et al 2005 [45], shows the values of the parameter q (L^2/pM^2) for various insulin analogues. Therefore, the parameter q for human insulin is estimated as the value for
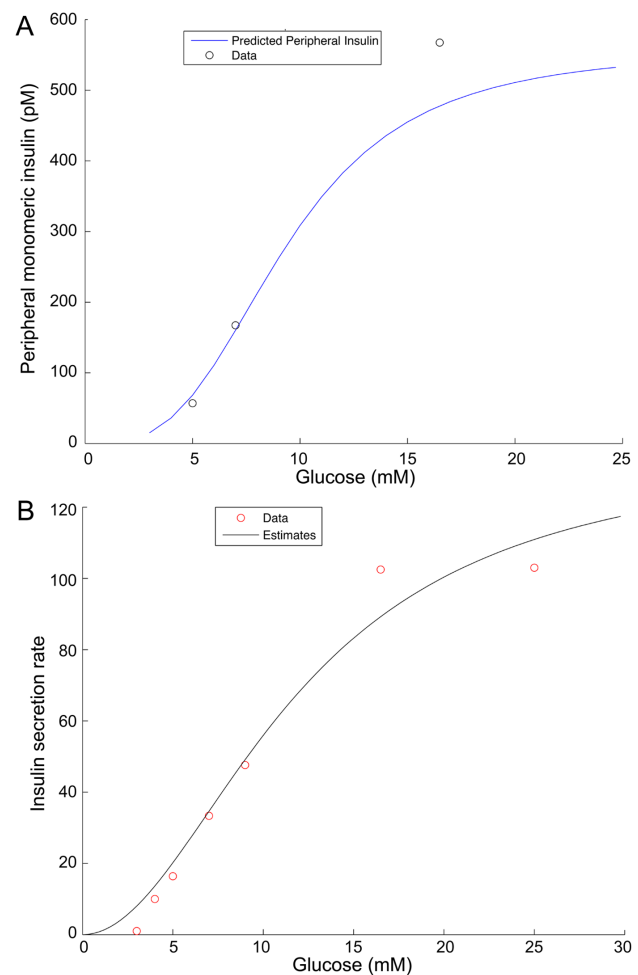
Figure 2. Validation of the model insulin secretion rate function. (**A**) The model output plotted against dose response data from Polonsky et al (1988) for comparison. (**B**) Insulin secretion rate data were use to estimate an insulin secretion rate response function. Model profiles were then created with different doses of clamped glucose (mM) and compared to peripheral insulin values (pM) at equilibrium at those glucose doses (mM).
doi:10.1371/journal.pone.0064860.g002

Semilente, i.e., $q=7.6\times10^{-2}$ ml^2/U$^2=1.6\times10^{-15}$ L^2/pmol^2 after unit conversion by a factor 2.1×10^{-14}.

The estimation of r and k was as follows. It is intuitive that it is faster for a dimer to dissolve to two monomers than for a hexamer to dissolve to three dimers. So it is reasonable to assume $r=\dfrac{3}{2}\times p=0.75$ min^{-1} and $k=\dfrac{2}{3}\times q=1.0\times10^{-15}$.

The estimation of d_i was as follows. Values for the degradation rate d_i of insulin have been reported within a wide range between 0.03–0.2 ([46]). To select a reasonable value for d_i, observing that in general a substrate decays exponentially, we considered the following ordinary differential equation,

$$I' = -d_i I, \quad I(0)=I_0,$$

where the initial condition represents the case of no secretion. The solution of this differential equation $I=I_0 e^{-d_i t}$ represents the change of amount of insulin over time. Notice that the half life of insulin is approximately in a range of 4–6 minutes [33]. Assuming

Table 1. Insulin secretion data rate and multiple glucose concentrations.

| Glucose level (mM)	Secretion rate (pM/min)	References and Notes
3	1	Data point estimated and added for fitting
4	10	Data point estimated and added for fitting
5	16	The case of overnight fast in [43]. Glucose level ranges between 4 and 6 mM after an overnight fast. We chose 5 mM.
7	33	The case of 24-h on mixed diet in [43]. We assume at 7 mM.
9	47	[44]
16.5	102	The case of hyperglycemic clamp at 16.5 mM in [43].
25	103	Data point estimated and added for fitting

doi:10.1371/journal.pone.0064860.t001

that the half-life of insulin is 6 min, when $t = 6$ min, $I = I_0/2$ and thus $I_0/2 = I_0 e^{-6d_i}$. Solving this equation for d_i yields $d_i = (\ln 2)/6 = 0.1$ min^{-1}.

The estimation of α was as follows. We estimated the parameter α (fraction coefficient of peripheral insulin) as follows. As expressed in equation (1), the rate of change of the returned peripheral insulin concentration in an islet, I', is affected by its degradation d_i and the concentration of newly secreted insulin monomers, M. Assume that x units of insulin monomers are secreted by a single islet. Thus, a total of x million units of insulin will be released into the portal vein from the one million islets of the pancreas, after which it becomes peripheral insulin. It is established that 50% of secreted insulin is removed from the circulation by the liver on the first pass. We assume an insulin degradation rate of $d_i = 0.1$ min^{-1} according to the estimation of d_i given above. Since it takes about 25 seconds for a complete circulation of blood, newly released insulin must return to the pancreas in the same time, where it is assumed to be evenly distributed among the one million islets. So, approximately $0.5x e^{-d_i T} = 0.48x$ units of insulin return to the same islet. Therefore, we estimate that $\alpha = 0.48$ min^{-1}.

Using our model with the above carefully selected parameter values, we simulated the dynamics of the various insulin concentrations at a range of clamped glucose concentrations. A stepwise increase in glucose from 0 mM to any value we tested resulted in an increase in peripheral insulin that reached a maximum in ~ 30 minutes (Fig. 3). As expected, the aggregated forms reached their peak faster. The concentration of monomeric insulin that has been newly release reaches only 100 pM after a jump to 15 mM glucose (a glucose concentration is much higher than what is seen in humans after a meal).

Importantly, we are able to use our model to estimate the total concentration of insulin monomers within the islet (i.e. newly made insulin + insulin returning from the periphery). By (3) and the parameter values we estimated above, we can derive the total monomeric insulin present in the islet at any glucose concentra-
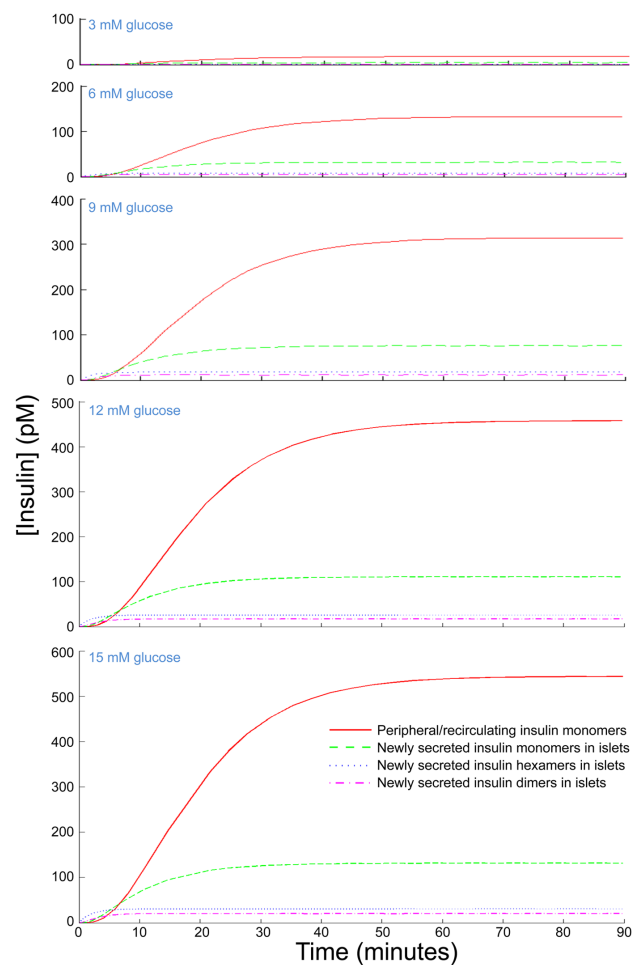
Figure 3. Numerical simulations of insulin hexamer, dimer and monomer concentration kinetics in a model human islet at multiple glucose concentrations. Profiles show the dynamics of the concentrations of newly synthesized insulin (in hexamer H, dimer D, monomer M) and returned peripheral insulin I and the equilibrium (H^*, D^*, M^*, I^*) (pM) at different clamped glucose inputs G_0 (mM).
doi:10.1371/journal.pone.0064860.g003

tion. Simple computation shows that $\sim 75\%$ of local monomeric insulin is peripheral insulin while $\sim 25\%$ is new monomeric insulin (Fig. 4). Our simulations clearly show that the majority of insulin in

Table 2. Values of parameter q for different insulin formulations.[1]

Units	Lispro	Actrapid	Semilente	NPH, Glargine
ml^2/U^2	4.8×10^{-4}	1.9×10^{-3}	7.6×10^{-2}	3.0
L^2/pmol^2	9.8×10^{-18}	3.9×10^{-17}	1.6×10^{-15}	6.3×10^{-14}

[1]This table is adopted from Table IV in Tarin et al [45].
doi:10.1371/journal.pone.0064860.t002

an islet is returned as monomeric peripheral insulin, whereas the newly secreted monomeric insulin from the islet provides a minor contribution in all cases tested. Therefore, our model predicts that the levels of insulin monomers in the islet do not exceed the picomolar range, even in extreme clamp studies (Fig. 4). Physiological meal-induced glucose excursions rarely fall outside the 4 mM to 8 mM range in normal humans, and our model suggests that monomeric insulin is unlikely to exceed 300 pM in these conditions (Fig. 4).

Model Validation

We validated the glucose-response component of our model by comparing the model-predicted values of glucose-stimulated insulin responses with the experimental data in [43]. The comparison is shown in Table 3 and Panel (A) in Fig. 2. It is well known that a swift increase of secretion occurs when glucose concentrations rise higher than fasting levels, but becomes saturated beyond the hyperglycemic range. No model can predict true physiology perfectly, but we suggest that this verification is valid because the response function of insulin secretion rate is obtained statistically according to the experimental data. The model-predicted dose response is in approximate agreement with the observed dose response in the same experiment. Some aspects of the model simulations, namely the exact concentration of monomeric insulin in the immediate vicinity of intact human islets *in vivo* must await the technology to measure this directly.

Proof of Theorem 1

Notice that the first three equations of model (1) do not involve I, hence we first consider the sub-model

$$\begin{cases} H'(t) = c - p(H(t) - qD^3(t)) \\ D'(t) = p(H(t) - qD^3(t)) - r(D(t) - kM(t)^2) \\ M'(t) = r(D(t) - kM(t)^2) - d_i M(t) \end{cases} \quad (5)$$

and then the original model (1).

The first quadrant of phase space is invariant. In fact, on the coordinate plane $H = 0$, $H' = c + pqD^3 > 0$; on $D = 0$, $D' = pH + rkM^2 \geq 0$; on $M = 0$, $M' = rD \geq 0$. Therefore, trajectories starting from the first quadrant will not cross any of the coordinate plane to negative side. We next construct a bounded region Ω (see Fig. 5) in the first quadrant such that the trajectory $\gamma(E_0)$ starting from $E_0 = (H(0), D(0), M(0)) \in \Omega$ will not cross the boundaries of Ω; that is, Ω is invariant, thus $\gamma(E_0)$ is bounded. We choose $a > \max\{H*, H(0)\}$ to be large. Let π_1 be the plane through the point $P_1(a, 0, 0)$ with the normal vector $(-1, 1, 1)$. Plane π_1 intersects the plane $D = D^*$ at the line $P_2 P_3$, where P_2 is on the plane $M = 0$ and P_3 is on the plane $M = M^*$. Let P_6 be the intersection point of the plane π_1, $D = 0$ and $M = M^*$. Thus $P_3 P_6$ is parallel to $P_1 P_2$, whose direction vector is $(1, 1, 0)$. Let π_2 be the plane passing through the line $P_2 P_3$ with the normal vector $(-1, -1, 1)$. Then π_2 intersects the plane $H = 0$ at the line $P_4 P_5$, where P_4 is on the plane $M = 0$, P_5 is on the plane $M = M^*$, and a is large enough so that the point $(H(0), D(0), 0)$ is on the same side of the line $P_2 P_4$ as the origin in the plane $M = 0$. Clearly the line $P_3 P_5$ is in the plane $M = M^*$. Let π_3 be the plane passing through the line $P_3 P_5$ with the normal vector $(-1, -1, -1)$, where we require that a was chosen large enough so that the point $(H(0), D(0), M(0))$ is on the same side of the plane π_3 as the origin. Let π_4 be the plane through the line $P_3 P_6$ and perpendicular to the plane $M = M^*$. Since $P_3 P_6$ is parallel to $P_1 P_2$ and the
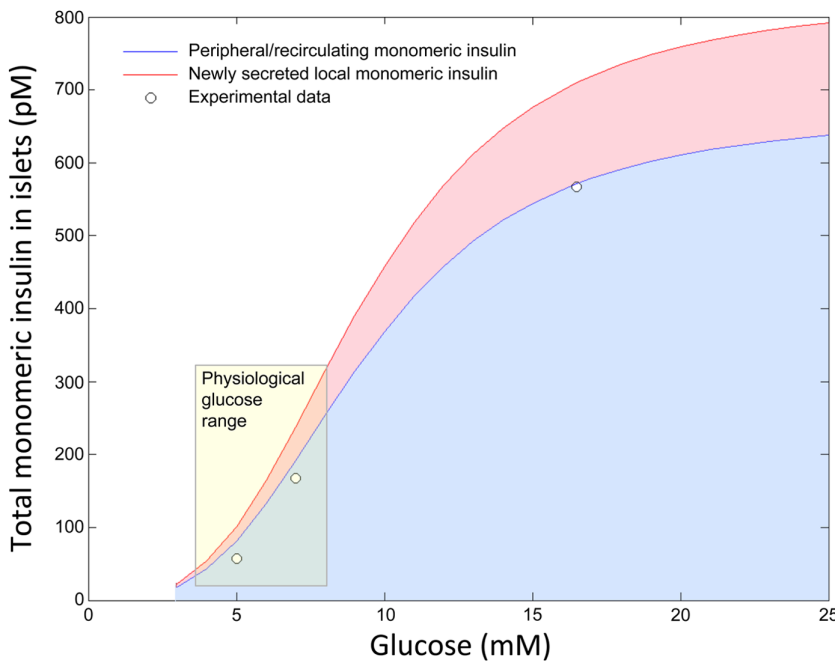
Figure 4. Total insulin monomer levels in a model islet resulting from the combination of new insulin and returning insulin. The dose-response relationship between glucose and total islet monomeric insulin. Newly released monomeric insulin (pink) plus returning peripheral monomeric insulin (blue) illustrates the total levels of monomeric insulin within islets. The white dots represent validation data from Polonsky et al 1988 ([43]).
doi:10.1371/journal.pone.0064860.g004

Table 3. Comparison of predicted dose-response and observed dose-response values.[1]

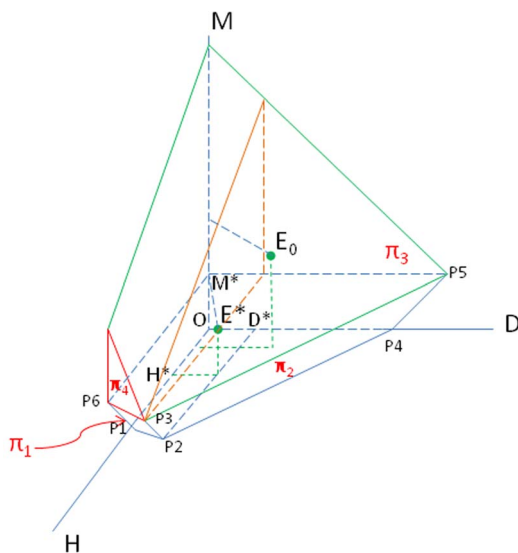| Glucose level (mM)	Predicted Peripheral Insulin (pM)	Observed Peripheral Insulin (pM)
5	77.7	57.0
7	186.3	167.4
16.5	571.5	567.4

[1]Data are from Polonsky et al 1988 [43].
doi:10.1371/journal.pone.0064860.t003

direction vector of P_1P_2 is $(1,1,0)$, the inward normal vector of π_4 is $(-1,1,0)$. Therefore, the planes π_i, $i=1,2,3,4$ and the coordinate planes $H=0, D=0, M=0$ form a closed region Ω (refer to Fig. 5), and $E_0 \in \Omega$.

Now we shall show that the bounded region Ω is invariant and thus $\gamma(E_0) \in \Omega$. To this end, we need only to show that the inner products of the inward normal vectors of the plane π_i, $i=1,2,3,4$, with the direction vector of trajectory starting from these planes are nonnegative.

On π_1, $M \leq M^*$, $D \leq D^*$ and $H \geq H^*$.

$$(H',D',M') \cdot (-1,1,1) = -H' + D' + M'$$

$$= -c + p(H-qD^3) + p(H-qD^3) - r(D-kM^2)$$

$$+ r(D-kM^2) - d_iM$$

$$= -c + 2p(H-qD^3) - d_iM$$

$$\geq -c + 2p(H-qD^3) - d_iM^*$$

$$= -2c + 2p(H-qD^3)$$

$$\geq -2c + 2p(H^* - qD^{*3})$$

$$= 2(-c + p(H^* - qD^{*3})) = 0.$$

On π_2, $D \geq D^*$ and $M \leq M^*$, thus we have

$$(H',D',M') \cdot (-1,-1,1) = -H' - D' + M'$$

$$= -c + p(H-qD^3) - p(H-qD^3) + r(D-kM^2)$$

$$+ r(D-kM^2) - d_iM$$

$$= -c + 2r(D-kM^2) - d_iM$$

$$\geq -c + 2r(D-kM^{*2}) - d_iM^*$$

$$= -2c + 2r(D-kM^{*2})$$

$$\geq -2c + 2r(D^* - kM^{*2})$$

$$= 2(-c + r(D^* - kM^{*2})) = 0.$$

On π_3, $M \geq M^*$, thus we have

$$(H',D',M') \cdot (-1,-1,-1) = -H' - D' - M'$$

$$= -c + p(H-qD^3) - p(H-qD^3) + r(D-kM^2)$$

$$- r(D-kM^2) + d_iM$$

Figure 5. The bounded region Ω for the proof of Theorem 1.
doi:10.1371/journal.pone.0064860.g005

$$= -c + d_i M \geq -c + d_i M^* = 0.$$

On π_4, $M \geq M^*$, $D \leq D^*$ and $H \geq H^*$, thus we have

$$(H',D',M') \cdot (-1,1,0) = -H' + D'$$

$$= -c + p(H - qD^3) + p(H - qD^3) - r(D - kM^2)$$

$$= -c + 2p(H - qD^3) - r(D - kM^2)$$

$$\geq -c + 2p(H^* - qD^{*3}) - r(D^* - kM^{*2})$$

$$= -c + 2c - c = 0.$$

Therefore these inner products are nonnegative, which implies the trajectory on boundaries π_i, $i = 1,2,3,4$ goes inward of Ω. Moreover, we have proved that the first quadrant is invariant (Theorem 1). Therefore, we conclude that Ω is invariant. It is equivalent to state that the solution to the sub-model 5 is bounded. Now for the model (1), since M is bounded, thus clearly I is bounded. We complete the proof.

Discussion

The goal of the present work was to estimate the local insulin concentrations within a working human pancreatic islet. This estimation is essential for efforts to understand the physiological relevance and mode of islet paracrine insulin signaling. More specifically, it has the potential to elucidate whether signaling is constitutive as a result of saturating local insulin levels or dynamic with monomeric insulin varying in a range that permits optimal activation of the insulin receptor. To the best of our knowledge, this is the first time any such estimation has been systematically generated. Our model suggests that locally produced insulin at steady state makes a relatively minor contribution to the local levels of monomeric insulin in an individual islet (estimated to be $\sim 25\%$). In contrast, the majority of locally available monomeric insulin within the islet derives from newly returned insulin from the peripheral circulation. Regardless, our model indicates that within an islet, the percentage of new insulin converted to monomers before being swept away by the blood flow is always less than the insulin returned from the peripheral circulation. Since the peripheral insulin concentration is well known, we can be confident that the total monomeric insulin concentration in the islet is not in orders of magnitude higher than it is in the periphery, as has been implied by some commentators. The model is dynamic, and our simulations show that the majority of the changes take place within 30 minutes, regardless of the glucose step. Since the initial conditions used in the simulations are somewhat arbitrary, one should not imply too much from the shape of these curves. Nevertheless, it is clear that the monomeric insulin concentration in the islet is relatively low in response to an increase in glucose at each time point before equilibrium is reached. It should also be noted that our model focuses primarily on glucose as the main stimulus for insulin release, and does not exclude modulatory contributions of other nutrients, incretin hormones or neural inputs, which increase insulin levels.

Many studies have investigated the effects of insulin on pancreatic β-cells; however, the vast majority have employed insulin doses in the high nanomolar range. This, together with culture conditions that allow insulin to accumulate, may be one of the reasons that some investigators have failed to observe significant effects of insulin in their *in vitro* experiments. Our model suggests that such high doses are non-physiological and up to ~ 1000 times higher than the locally present levels. Importantly, nanomolar doses of insulin would maximally stimulate IGF1 receptors [47], which do not play an essential role in islet survival and have only a minor role on β-cell function [5],[48]. Our model also suggests that the concentration of free monomeric insulin in the islet may not exceed ~ 300 pM while glucose is in the physiological range. Thus, local autocrine/paracrine insulin signaling is likely to be dynamic and physiologically relevant in the picomolar range. This also means the experimentally defined 'sweet spot' where β-cells respond *in vitro* optimally to picomolar insulin is likely to be well within the *in vivo* physiological range [1]. This might seem counterintuitive, but our model suggests that the slow kinetics by which insulin crystals dissolve keeps the local monomeric insulin levels surprisingly low. Although we have not considered the rate of islet blood flow in our model, it may nonetheless be important and should be considered in future models. Changes in islet vasculature and/or blood flow might therefore represent physiological and pathological modes of altering local insulin signaling.

One important assumption of our model is that the percentage of insulin released in its crystalized form is high. This generally appears to be well supported by the literature, but there are cases where it might not be as assumed here. Some species of rodents (e.g. porcupines) have insulin genes with alterations in amino acids known to be important in zinc binding and crystal formation [49]. In these examples, we might therefore expect an increased ratio of monomeric to hexameric local insulin and possibly a desensitization of islet insulin signaling, but this should be investigated in future modeling studies. Similarly, a human mutation (AspB10) has been described that alters insulin binding to zinc and complex assembly, and we would predict that autocrine insulin signaling might be altered in such patients, in addition to multiple other defects [50]. It would also be interesting to determine if modifications in insulin packaging caused by recently described genetic polymorphisms in zinc transporters might affect the ratio of insulin released in a post-crystalized form under specific conditions [51]. In each of these cases, we expect insulin signaling pathways to compensate in the face of altered monomeric insulin levels [52].

We speculate that our findings also have implications for efforts to understand the evolution and function of the endocrine pancreas. Remarkably, the size of islets is relatively similar between mammals of different body sizes, with the total number of islets varying between small and large species. The islets of Langerhans are also somewhat unique as an endocrine organ in that they are spread throughout the large pancreas in a diffuse, but non-random manner. We speculate that this architecture evolved to prevent the accumulation of high levels of insulin in and around the islets. Insulin is a powerful mitogen [53] and we have shown it can stimulate primary islet cell proliferation [15]. We have recently shown that pancreatic insulin hypersecretion is required for the increase in islet size observed during high fat feeding [9]. Thus, the diffuse distribution of relative small islets might be evolutionarily conserved to prevent excessive local insulin concentrations that might increase the risk of pancreatic cancer.

Indeed, significant molecular, clinical and epidemiological findings point to important links between hyperinsulinemia and pancreatic cancer [54], [55], [56], [57], [58].

This work is the first to model the intra-islet concentration of monomeric islet insulin. We conclude that the major contributor to the human islet insulin levels is peripheral insulin owing to the relatively slow dissolution of newly secreted insulin crystals. We find that the total concentration of free monomeric insulin, capable of activating the insulin receptor, remains in the picomolar range regardless of glucose stimulation. Together, these findings add novel insight into pancreatic islet biology and provide

context to the experimental studies focused on the effects of islet insulin signaling. Our work helps contextualize *in vivo* and *in vitro* studies on the autocrine effects of insulin and lay the groundwork for future mathematical and physiological studies.

Author Contributions

Conceived and designed the experiments: JL JDJ. Performed the experiments: MW. Analyzed the data: MW. Wrote the paper: MW JL GEL JDJ.

References

1. Johnson JD, Alejandro EU (2008) *Control of pancreatic beta-cell fate by insulin signaling: The sweet spot hypothesis*, Cell Cycle 7: 1343–1347.

2. Leibiger IB, Leibiger B, Berggren PO (2008) *Insulin signaling in the pancreatic beta-cell*, Annu Rev Nutr 28: 233–251.

3. Gunton JE, Kulkarni RN, Yim S, Okada T, Hawthorne WJ, et al. (2005) *Loss of ARNT/HIF1beta Mediates Altered Gene Expression and Pancreatic-Islet Dysfunction in Human Type 2 Diabetes*, Cell 122: 337–349.

4. Kulkarni RN, Bruning JC, Winnay JN, Postic C, Magnuson MA, et al. (1999) *Tissue-specific knockout of the insulin receptor in pancreatic beta cells creates an insulin secretory defect similar to that in type 2 diabetes*, Cell 96: 329–339.

5. Kulkarni RN, Holzenberger M, Shih DQ, Ozcan U, Stoffel M, et al. (2002) *Beta-cell-specific deletion of the Igf1 receptor leads to hyperinsulinemia and glucose intolerance but does not alter beta-cell mass*, Nat Genet 31: 111–115.

6. Ueki K, Okada T, Hu J, Liew CW, Assmann A, et al. (2006) *Total insulin and IGF-I resistance in pancreatic beta cells causes overt diabetes*, Nat Genet 38: 583–588.

7. Ueki K, Okada T, Ozcan U, Kulkarni R (2003) *Endogenous insulin-mediated signaling protects apoptosis induced by glucose in pancreatic beta-cells*, Diabetes 52: A42–A42.

8. Okada T, Liew CW, Hu J, Hinault C, Michael MD, et al. (2007) *Insulin receptors in beta-cells are critical for islet compensatory growth response to insulin resistance*, Proc Natl Acad Sci U S A 104: 8977–8982.

9. Mehran AE, Templeman NM, Brigidi GS, Lim GE, Chu KY, et al. (2012) *Hyperinsulinemia drives diet-induced obesity independently of brain insulin production*, Cell Metabolism 16: 723–737.

10. Li X, Zhang L, Meshinchi S, Dias-Leme C, Raffin D, et al. (2006) *Islet microvasculature in islet hyperplasia and failure in a model of type 2 diabetes*, Diabetes 55: 2965–2973.

11. Johnson JD, Misler S (2002) *Nicotinic acid-adenine dinucleotide phosphate-sensitive calcium stores initiate calcium signaling in human beta cells*, Proc Natl Acad Sci U S A 99: 14566–14571.

12. Alejandro EU, Kalynyak TB, Taghizadeh F, Gwiazda KS, Rawstron EK, et al. (2010) *Acute insulin signaling in pancreatic beta-cells is mediated by multiple Raf-1 dependent pathways*, Endocrinology 151: 502–512.

13. Alejandro EU, Johnson JD (2008) *Inhibition of raf-1 alters multiple downstream pathways to induce pancreatic beta-cell apoptosis*, Journal of Biological Chemistry 283: 2407–2417.

14. Lim GE, Piske M, Johnson JD (2013) *14-3-3 proteins are essential signalling hubs for beta cell survival*, Diabetologia.

15. Beith JL, Alejandro EU, Johnson JD (2008) *Insulin stimulates primary beta-cell proliferation via Raf-1 kinase*, Endocrinology 149: 2251–2260.

16. Bouche C, Lopez X, Fleischman A, Cypess AM, O'Shea S, et al. (2010) *Insulin enhances glucose-stimulated insulin secretion in healthy humans*, Proc Natl Acad Sci U S A 107: 4770–4775.

17. Luciani DS, Johnson JD (2005) *Acute effects of insulin on beta-cells from transplantable human islets*, Molecular and Cellular Endocrinology 241: 88–98.

18. Johnson JD, Ford EL, Bernal-Mizrachi E, Kusser KL, Luciani DS, et al. (2006) *Suppressed insulin signaling and increased apoptosis in CD38-null islets*, Diabetes 55: 2737–2746.

19. Song SH, McIntyre SS, Shah H, Veldhuis JD, Hayes PC, et al. (2000) *Direct measurement of pulsatile insulin secretion from the portal vein in human subjects*, J Clin Endocrinol Metab 85: 4491–4499.

20. Saisho Y, Butler AE, Meier JJ, Monchamp T, Allen-Auerbach M, et al. (2007) *Pancreas volumes in humans from birth to age one hundred taking into account sex, obesity, and presence of type-2 diabetes*, Clin Anat 20: 933–942.

21. Nyman LR, Wells KS, Head WS, McCaughey M, Ford E, et al. (2008) *Real-time, multidimensional in vivo imaging used to investigate blood ow in mouse pancreatic islets*, J Clin Invest.

22. Michael DJ, Ritzel RA, Haataja L, Chow RH (2006) *Pancreatic beta-cells secrete insulin in fast- and slow-release forms*, Diabetes 55: 600–607.

23. Whittaker L, Hao C, Fu W, Whittaker J (2008) *High-a nity insulin binding: insulin interacts with two receptor ligand binding sites*, Biochemistry 47: 12900–12909.

24. Li JX, Johnson JD (2009) *Mathematical Models of Subcutaneous Injection of Insulin Analogues: A Mini-Review*, Discrete and Continuous Dynamical Systems-Series B 12: 401–414.

25. Misler S, Barnett DW, Gillis KD, Pressel DM (1992) *Electrophysiology of Stimulus-Secretion Coupling in Human Beta-Cells*, Diabetes 41: 1221–1228.

26. Soeborg T, Rasmussen CH, Mosekilde E, Colding-Jorgensen M (2009) *Absorption kinetics of insulin after subcutaneous administration*, Eur J Pharm Sci 36: 78–90.

27. Li J, Kuang Y (2009) *Systemically modeling the dynamics of plasma insulin in subcutaneous injection of insulin analogues for type 1 diabetes*, Math Biosci Eng 6: 41–58.

28. Mosekilde E, Jensen KS, Binder C, Pramming S, Thorsteinsson B (1989) *Modeling absorption kinetics of subcutaneous injected soluble insulin*, J Pharmacokinet Biopharm 17: 67–87.

29. Johnson JD, Ahmed NT, Luciani DS, Han Z, Tran H, et al. (2003) *Increased islet apoptosis in Pdx1+/− mice*, J Clin Invest 111: 1147–1160.

30. Cabrera O, Berman DM, Kenyon NS, Ricordi C, Berggren PO, et al. (2006) *The unique cytoarchitecture of human pancreatic islets has implications for islet cell function*, Proceedings of the National Academy of Sciences of the United States of America 103: 2334–2339.

31. Pisania A, Weir GC, O'Neil JJ, Omer A, Tchipashvili V, et al. (2010) *Quantitative analysis of cell composition and purity of human pancreatic islet preparations*, Laboratory investigation; a journal of technical methods and pathology 90: 1661–1675.

32. Trajanoski Z, Wach P, Kotanko P, Ott A, Skraba F (1993) *Pharmacokinetic model for the absorption of subcutaneously injected soluble insulin and monomeric insulin analogues*, Biomed Tech (Berl) 38: 224–231.

33. Matthews DR, Rudenski AS, Burnett MA, Darling P, Turner RC (1985) *The half-life of endogenous insulin and C-peptide in man assessed by somatostatin suppression*, Clinical Endocrinology 23: 71–79.

34. Meier JJ, Butler AE, Saisho Y, Monchamp T, Galasso R, et al. (2008) *Beta-cell replication is the primary mechanism subserving the postnatal expansion of beta-cell mass in humans*, Diabetes 57: 1584–1594.

35. Lammert E, Gu G, McLaughlin M, Brown D, Brekken R, et al. (2003) *Role of VEGF-A in vascularization of pancreatic islets*, Curr Biol 13: 1070–1074.

36. Miles KA, Hayball MP, Dixon AK (1995) *Measurement of human pancreatic perfusion using dynamic computed tomography with perfusion imaging*, The British journal of radiology 68: 471–475.

37. Palumbo P, Panunzi S, De Gaetano A (2007) *Qualitative behavior of a family of delay-differential models of the glucose-insulin system*, Discrete and Continuous Dynamical Systems-Series B 7: 399–424.

38. Panunzi S, Palumbo P, De Gaetano A (2007) *A discrete Single Delay Model for the Intra-Venous Glucose Tolerance Test*, Theor Biol Med Model 4: 35.

39. Li J, Wang M, DeGaetano A, Palumbo P, Panunzi S (2012) *The range of time delay and the global stability of the equilibrium for an IVGTT model*, Math Biosc 235: 128–137.

40. Li JX, Kuang Y, Mason CC (2006) *Modeling the glucose-insulin regulatory system and ultradian insulin secretory oscillations with two explicit time delays*, Journal of Theoretical Biology 242: 722–735.

41. Sturis J, Polonsky KS, Mosekilde E, Vancauter E (1991) *Computer-Model for Mechanisms Underlying Ultradian Oscillations of Insulin and Glucose*, American Journal of Physiology 260: E801–E809.

42. Smith HL (1995) *Monotone Dynamical Systems, an Introduction to the Theory of Competitive and Cooperative Systems*.

43. Polonsky KS, Given BD, Hirsch L, Shapiro ET, Tillil H, et al. (1988) *Quantitative Study of Insulin Secretion and Clearance in Normal and Obese Subjects*, Journal of Clinical Investigations 81: 435–441.

44. Jones CN, Pei D, Staris P, Polonsky KS, Chen YD, et al. (1997) *Alterations in the glucose-stimulated insulin secretory dose-response curve and in insulin clearance in nondiabetic insulin-resistant individuals*, The Journal of clinical endocrinology and metabolism 82: 1834–1838.

45. Tarin C, Teufel E, Pico J, Bondia J, Pfleiderer HJ (2005) *Comprehensive pharmacokinetic model of insulin Glargine and other insulin formulations*, IEEE Trans Biomed Eng 52: 1994–2005.

46. Engelborghs K, Lemaire V, Belair J, Roose D (2001) *Numerical bifurcation analysis of delay differential equations arising from physiological modeling*, Journal of Mathematical Biology 42: 361–385.

47. De Meyts P, Whittaker J (2002) *Structural biology of insulin and IGF1 receptors: implications for drug design*, Nat Rev Drug Discov 1: 769–783.

48. Kulkarni RN (2005) New insights into the roles of insulin/IGF-I in the development and maintenance of beta-cell mass, Rev Endocr Metab Disord 6: 199–210.

49. Horuk R, Blundell TL, Lazarus NR, Neville RW, Stone D, et al. (1980), *A monomeric insulin from the porcupine (Hystrix cristata), an Old World hystricomorph*, Nature 286: 822–824.

50. Carroll RJ, Hammer RE, Chan SJ, Swift HH, Rubenstein AH, et al. (1988), *A mutant human proinsulin is secreted from islets of Langerhans in increased amounts via an unregulated pathway*, Proceedings of the National Academy of Sciences of the United States of America 85: 8943–8947.

51. Lemaire K, Ravier MA, Schraenen A, Creemers JW, Van de Plas R, et al. (2009), *Insulin crystallization depends on zinc transporter ZnT8 expression, but is not required for normal glucose homeostasis in mice*, Proceedings of the National Academy of Sciences of the United States of America 106: 14872–14877.

52. Horuk R, Goodwin P, O'Connor K, Neville RW, Lazarus NR, et al. (1979), *Evolutionary change in the insulin receptors of hystricomorph rodents*, Nature 279: 439–440.

53. Ish-Shalom D, Christoffersen CT, Vorwerk P, Sacerdoti-Sierra N, Shymko RM, et al. (1997), *Mitogenic properties of insulin and insulin analogues mediated by the insulin receptor*, Diabetologia 40 Suppl 2: S25–31.

54. Fisher WE, Boros LG, Schirmer WJ (1996), *Insulin promotes pancreatic cancer: evidence for endocrine inuence on exocrine pancreatic tumors*, J Surg Res 63: 310–313.

55. Gullo L (1999), *Diabetes and the risk of pancreatic cancer*, Ann Oncol 10 Suppl 4: 79–81.

56. Evert M, Sun J, Pichler S, Slavova N, Schneider-Stock R, et al. (2004), *Insulin receptor, insulin receptor substrate-1, Raf-1, and Mek-1 during hormonal hepato-carcinogenesis by intrahepatic pancreatic islet transplantation in diabetic rats*, Cancer Res 64: 8093–8100.

57. Currie CJ, Poole CD, Gale EA (2009), *The inuence of glucose-lowering therapies on cancer risk in type 2 diabetes*, Diabetologia 52: 1766–1777.

58. Li D, Yeung SC, Hassan MM, Konopleva M, Abbruzzese JL (2009), *Antidiabetic therapies affect risk of pancreatic cancer*, Gastroenterology 137: 482–488.